INTERNATIONAL ATOMIC ENERGY AGENCY
UNITED NATIONS EDUCATIONAL, SCIENTIFIC AND CULTURAL ORGANIZATION
INTERNATIONAL CENTRE FOR THEORETICAL PHYSICS
I.C.T.P., P.O. BOX 586, 34100 TRIESTE, ITALY, CABLE: CENTRATOM TRIESTE

UNITED NATIONS INDUSTRIAL DEVELOPMENT ORGANIZATION

INTERNATIONAL CENTRE FOR SCIENCE AND HIGH TECHNOLOGY
c/o INTERNATIONAL CENTRE FOR THEORETICAL PHYSICS 34100 TRIESTE (ITALY) VIA GRIGNANO, 9 (ADRIATICO PALACE) P.O. BOX 586 TELEPHONE 040-224572 TELEFAX 040-224575 TELEX 460449 APH I

H4.SMR/676-27

**SECOND SCHOOL ON THE USE OF SYNCHROTRON RADIATION IN SCIENCE AND TECHNOLOGY:**
***"JOHN FUGGLE MEMORIAL"***

**25 October - 19 November 1993**

***Miramare - Trieste, Italy***

***Section:***

***X-ray Diffraction Applied to Material Science Organization***

**A. Craievich**
**National Laboratory for Synchrotron Radiation**
**(LNLS)**
**Campinas, Brazil**



## Section: X-ray Diffraction Applied to Material Science

## Organization

i) Single Crystal Crystallography
Applied to inorganic materials
(Collapietro, Rome)

ii) "Perfect Crystal" Crystallography
- Dynamical theory of X-ray diffraction
- Application to standing wave technique

(Tolentino, Campinas)

iii) X-ray Scattering by Imperfect, Amorphous and Heterogeneous Solids
- Basic kinematical theory of X-ray diffraction
- Difuse scattering by imperfect solids
- X-ray diffraction by amorphous materials
- Small Angle X-ray Scattering (SAXS) by heterogeneous materials

(Craievich, Campinas)

## Tutorial 1

SAXS applications

i) Basic calculations
ii) Nanocrystal formation in glasses
iii) Fractal systems

(Craievich, Campinas)

## Tutorial 2

i) Single crystal crystallography instrumentation

(Collapietro, Rome)

ii) SAXS study of phase separation

(Craievich, Campinas)

## X-ray Scattering by Imperfect, Amorphous and Heterogeneous Solids

I) Basic kinematical of X-ray scattering by imperfect solids

- Ideal and real atoms strcutures of crystalline and amorphous solids
- Concepts of reciprocal space
- Ewald sphere
- Diffraction by "perfect" and "imperfect" crystals
- Anomalous scattering
- Short range order in single crystals
- Scattering by polycrystals (powders)

## X-ray Diffraction References

### A) Basic Aspects


- A. Guinier, Diffraction of X-rays
- B. Warren, X-ray Diffraction
- O. Glatter and O. Kratky, Small Angle X-ray Scattering


### B) X-ray Diffraction by Polycrystalline Solids


- Instrumentation and methods for powder diffraction with synchrotron radiation, T. Wroblewski, Acta Physica Polonica A, 82, 67 (1992).

- J. Ihringer, A. Küster, J. K. Maichle, T. Wroblewski, J. Appl. Cryst., 21, 972 (1988).


### C) Wide-angle X-ray Scattering by Amorphous Solids


- J. C. de Lima, J. M. Tonerre and D. Raoux, J. Non-Cryst. Solids 106, 38 (1988).

- A method for determination of partial structure factors of binary amorphous alloys. G. H. Bezerra, L. Q. Amaral, A. F. Craievich and D. Raoux, J. Non-Cryst. Solids, 126, 239 (1990).

- J. C. de Lima, D. Raoux, Y. Charreire and M. Maurer, J. Phys. Chem., 157, 65 (1988).


### D) Small-angle X-ray Scattering by Heterogeneous Materials


- Particle size distribution from small-angle scattering data. G. Walter, R. Kranold, Th. Gerber, J. Baldrian and M. Steinhat, J. Appl. Cryst., 18, 205 (1985).

- Small-angle scattering by fractal systems. J. Teixeira, J. Appl. Cryst., 21, 781 (1988).

- Scattering from fractals. J. E. Martin and A. J. Hurd, J. Appl. Cryst., 20, 61 (1987).

- SAXS studies of phase separation in borate glasses and structural transformation in precursor of silica glass. A. Craievich, J. de Physique, 2, 801 (1992).

• SAXS study of growth kinetic of fractal aggregates in TEOS-water-alcohol solutions with formamide. E. Blanco, M. Ramirez del Solar, N. de la Rosa-Fox and A. Craievich, J. Non-Cryst. Solids, 147-148, 238 (1992).

• A small angle X-ray scattering workstation for the National Laboratory for Synchrotron Light. L. A. Bernardes, H. Tolentino, A. R. D. Rodrigues, A. Craievich and I. Torriani, Rev. Scient. Instrum. 63, 1065 (1992).

## Reciprocal Space

From the vectors which define the unit cell ($\vec{a}$, $\vec{b}$, $\vec{c}$) of the lattice points associated with the atomic structure of solids, a reciprocal lattice can be deduced as follows:

$$\left.\begin{aligned} \vec{a}^{*} &= \frac{\vec{b}\times\vec{c}}{V_c} \\ \vec{b}^{*} &= \frac{\vec{c}\times\vec{a}}{V_c} \\ \vec{c}^{*} &= \frac{\vec{a}\times\vec{b}}{V_c} \end{aligned}\right\}$$

where $V_c$ is the volume of the unit cell.

From 1 it follows that:

$$\vec{a}^* \perp \vec{a}, \vec{b}$$

$$\vec{b}^* \perp \vec{c}, \vec{a}$$

$$\vec{c}^* \perp \vec{a}, \vec{b}$$

$$\vec{a}^* \, \vec{a} = 1 \ , \ldots$$

$$a^* \, \vec{b} = 0 \ , \ldots$$

$$V_c^* = V_c = 1$$

The reciprocal lattice is defined by

$$\vec{r}^*_{hk\ell} = h\,\vec{a}^* + k\,\vec{b}^* + \ell\,\vec{c}^*$$

The reciprocal lattice of points is defined in the reciprocal space.

Bragg law in reciprocal space:

($2d \operatorname{sen} \theta = \lambda$; $\theta_i = \theta_r$)

$$\boxed{\vec{s} = \vec{r}^*_{hk\ell}}$$

Ewald sphere

$$\vec{s} = \frac{\vec{S}}{\lambda} - \frac{\vec{S}_o}{\lambda}$$

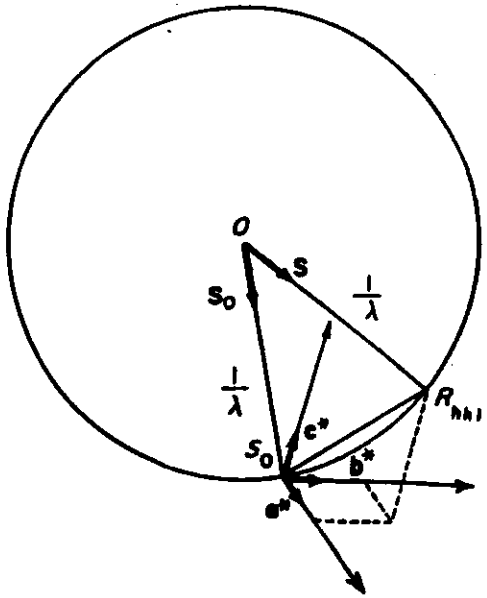


Atomic factor: $$f(\vec{s}) = \frac{A(\vec{s})\,(atoms)}{a_e\,(electrons)}$$

$$f(\vec{s}) = \int \rho(\vec{r})\, e^{2\pi i\, \vec{s}.\vec{r}}\, d\vec{r}$$

Structure factor: $$F_{hk\ell} = \frac{A_{hk\ell}\,(unit\ cell)}{A_{hk\ell}\,(atom)}$$

$$F_{hk\ell} = \sum f_j(s)\, e^{2\pi i(hu_j + kv_j + \ell w_j)}$$

where h, k,$\ell$ indicate the reciprocal lattice point and $u_j$, $v_j$, $w_j$ are the fractional coordinates of the atom constituting the basis of the structure.

The total amplitude of the scattering by N unit cells is given by

$$A_{hk\ell} = Na_e\, F_{hk\ell}$$

$$\rho(x,y,z) = \sum A_{hk\ell}\, e^{2\pi i(hx+ky+\ell z)}$$

$$= Na_e \sum F_{hk\ell}\, e^{2\pi i(hu_j+kv_j+\ell w_j)}$$

Imperfect crystals

$$F(\vec{s}) = \sum f_r \, e^{-2\pi i \vec{s}\,\vec{x}_r}$$

$$F_n(\vec{s}) = \sum f_{nr} \, e^{-2\pi i \vec{s}\,\vec{x}_r}$$

$$I_N(\vec{s}) = \sum_n \sum_{n'} F_n \, F_{n'}^* \, e^{-2\pi i \vec{s}(\vec{x}_n - \vec{x}_{n'})}$$

$$I_N(\vec{s}) = \sum_m (\sum_m F_n \, F_{n+m}^*) \, e^{2\pi i \vec{s}\,\vec{x}_m}$$

$$\overline{F_n \, F_{n+m}^*} = \frac{1}{p} \sum_n F_n \, F_{n+m}^* = Y_m$$

$$\sum_n F_n \, F_{n+m}^* = N' \, Y_m$$

where $N' = \dfrac{V(\vec{x}_m)}{\dot{v}_1} = NV(\vec{x}_m)$

$\therefore$

$$I_N(s) = N \sum_m y_m \, V(\vec{x}_m) \, e^{2\pi i \vec{s}\,\vec{x}_m}$$

for large crystals:

$$I_N(s) = N \sum_m Y_m \, e^{2\pi i \vec{s}\,\vec{x}_m}$$

$$I(s) = \sum_m Y_m \, e^{2\pi i \vec{s}\,\vec{x}_m}$$

$$\overline{F} = \frac{1}{N} \sum_n F_n$$

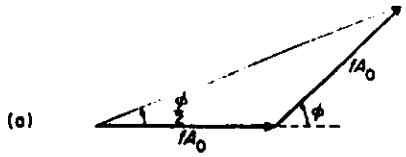


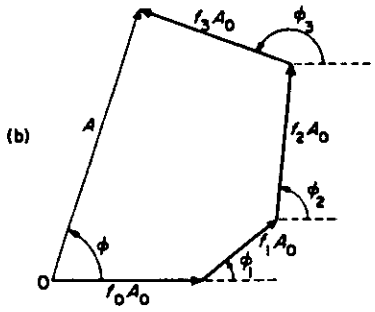


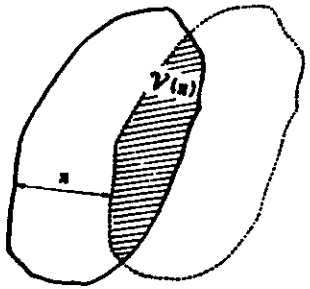


$$\therefore F_n = \overline{F} + \varphi_n$$

$$Y_m = \overline{F_n\, F^*_{n+m}} = \overline{(\overline{F} + \varphi_n)(\overline{F^*} + \varphi^*_{n+m})}$$

$$= \overline{F}\,\overline{F^*} + \overline{F}\,\overline{\varphi^*_{n+m}} + \overline{F^*}\,\overline{\varphi_n} + \overline{\varphi_n\,\varphi^*_{n+m}}$$

$$\| \qquad\qquad \|$$
$$0 \qquad\qquad 0$$

$$\therefore Y_m = |\overline{F}|^2 + \overline{\varphi_n\,\varphi^*_{n+m}} = |\overline{F}|^2 + \phi_m$$

$$\underline{I(\vec{s})} = |\overline{F}|^2 \sum e^{2\pi i \vec{s}\,\vec{x}_m} + \sum \underline{\phi_m}\, e^{2\pi i \vec{s}\,\vec{x}_m}$$

$$= I_1(s = r^*_{hk\ell}) + I_2(\vec{s})$$

$$\boxed{I_2(s) = \sum \phi_m\, e^{2\pi i \vec{s}\,\vec{x}_m}}$$

Laue scattering <-> no correlations

$\phi_m \neq 0$ if $m = 0$

$$\therefore\ I_2(s) = \phi_o = \overline{\varphi_n\ \varphi_n^*} = \overline{|F|^2} - |\overline{F}|^2$$

$$\phi_m = v_1 \int I_2(s)\, e^{-2\pi i\, \vec{s}\ \vec{x}_m}\ dv_s$$

Planar disorder

Linear disorder

Displacement disorder

- Thermal diffuse scattering

$$I(\vec{s}) = \frac{f^2\ \pi^2}{V_c}\, s^2 \sum_i A_i^2 \cos^2 \alpha_i$$

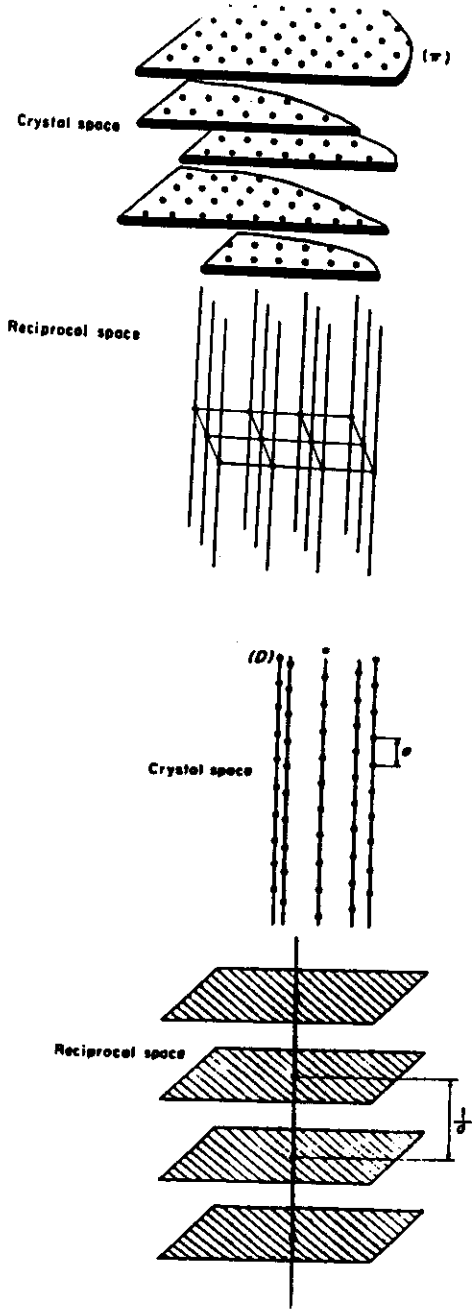


Substitutional disorder

- Short range order and aggregation

α: order parameter

$$\phi_m = C_A\, C_B (f_A - f_B)^2\, \alpha_m$$

$$\alpha_m = 1 - \frac{n_{AB}}{C_B}$$

Short
range
order

$$I_2(\vec{s}) = \sum \phi_m \, e^{2\pi i \vec{s}\,\vec{x}_m}$$

$$I_2(\vec{s}) = C_A \, C_B (f_A - f_B)^2 \sum \alpha_m \, e^{2\pi i \vec{s}\,\vec{x}_m}$$

$$\alpha_m = \int_{cell} \frac{I_2(\vec{s})}{C_A \, C_B (f_A - f_B)^2} \, e^{-2\pi i \vec{s}\,\vec{x}_m} \, dV_s$$

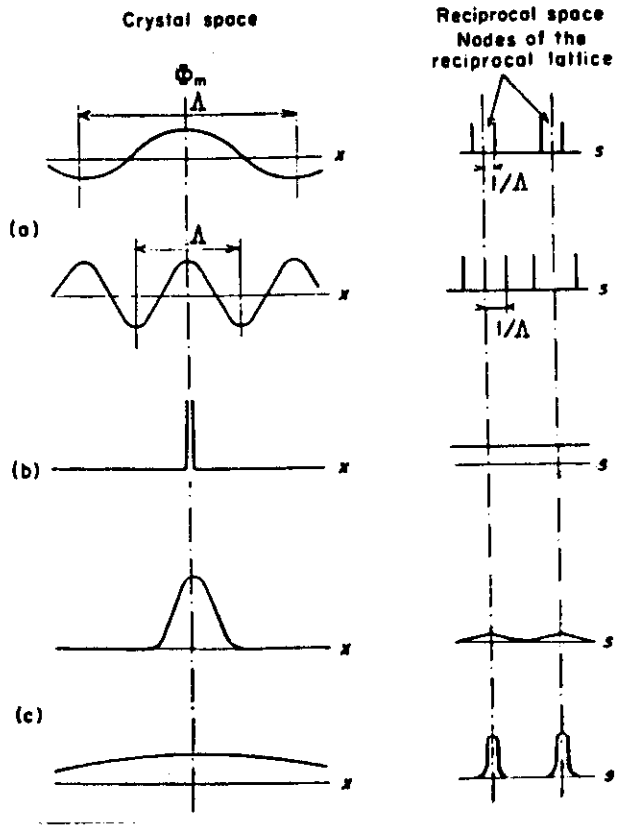

X-ray scattering outside the reciprocal lattice points is associated with structure imperfections

- Scattering within lines of reciprocal space is related to planar disorder in the structure

- Scattering on planes of reciprocal space is related to linear disorder in the structure

- Scattering which is not periodic in reciprocal space and increase for high s is associated with displacement structure disorder

- Quasi-periodic scattering in reciprocal space is associated with substitutional disorder.

i) Scattering concentrated close to the points of the reciprocal lattice points is connected with segregation

ii) Scattering concentrated far from the reciprocal lattice points is connected with short range order

- Small angle scattering (SAXS) is sensitive to segregation. Displacement disorder does not contribute to SAXS

- All this theory applied to structure which can be described by a model based on an average structure and deviations from it. Amorphous materials does not exhibit a periodic behavior. In this case Bragg reflections are not observed and the scattering is continuous throught the reciprocal space. Isotropic amorphous materials are characterized by a I(s) function which is isotropic in the reciprocal space.

Determination of crystal size

$$L = \frac{0{,}9\lambda}{\cos\theta_o \, \Delta(2\theta)}$$

$$i_1(s) = \int i(s_1)\, i_o(s - s_1)\, ds$$

↓ ↓ ↓

experiment — intensity profile without instrumental contribution — instrument

Powder method

The scattering power for crystalline powders is given by:

$$I = I_o \, r_e^2 \, \frac{1 + \cos^2 2\theta}{2} \, \frac{1}{16\pi \, r \, sen^2\theta \cos\theta} \cdot$$

$$\lambda^3 \, F_{hk\ell}^2 \, n \frac{1}{V_c^2} \, D \, dV$$

I: Scattering power per unit length in Debye-Scherrer patterns recorded at a distance r from the sample.

$I_o$: Incident X-ray intensity (per surface unit of the incoming beam)

θ: Bragg angle

$\frac{1+\cos^2 2\theta}{2}$ : polarization factor

$\frac{1}{sen^2\theta\cos\theta}$ : Lorentz factor (comes from the characteristic geometry for Debye-Scherrer patterns)

$F_{hk\ell}$: structure factor

n: multiplicity factor

$V_c$: volume of the unit cell

D: Debye-Waller factor

dV: volume of the sample

Bragg-Brentano geometry

$$I = SI_o\, r_e^2\, \frac{1}{32\pi r}\, \frac{\lambda^3}{V_c^2}\, F_{hk\ell}^2\, n\, \frac{1+\cos^2 2\theta}{sen^2\cos\theta}\, D\, \frac{1}{2\mu\rho}$$

Precise determination of lattice parameters

$\lambda = 2d\ sen\theta$

$$\frac{\Delta\lambda}{\lambda} = \frac{2\,\Delta d\ sen\theta}{2d\,sen\theta} + \frac{2d\cos\theta\,\Delta\theta}{2d\ sen\theta}$$

$$\boxed{\frac{\Delta d}{d} = -ctg\theta\,\Delta\theta} \qquad \frac{\Delta d}{d} \to 0 \text{ for } 2\theta \equiv \pi$$

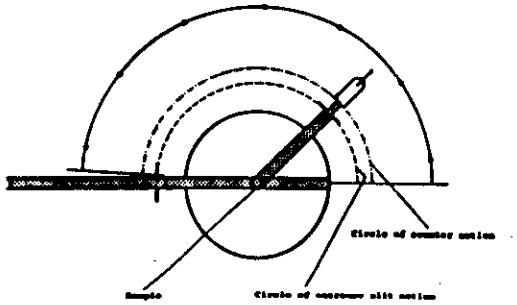

Figure 2: With a parallel monochromatic beam and a stationary entrance slit the machine can operate as a Debye-Scherrer diffractometer.

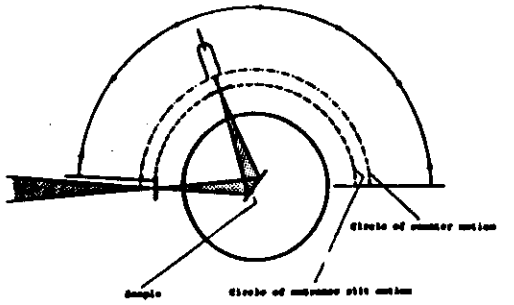

Figure 3: With a divergent monochromatic beam and a stationary entrance slit a Bragg-Brentano diffractometer is obtained. The motion of the sample and that of the detector must be coupled by a ratio 1:2.

Cox et.al. 1983

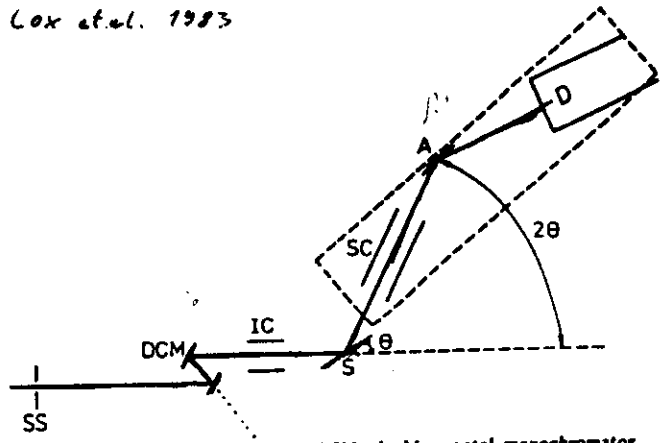


*Beam path: SS = slit system, DCM = double crystal monochromator IC = ionisation chamber monitor, S = sample, SC = Soller collimator (horizontal), A = analyser crystal, D = detector*

$$FWHM^2 = \Delta_A^2 + (2tg\theta - 2tg\theta_M - tg\theta_A)^2 (\Delta_M / tg\theta_M)^2 + (2tg\theta - tg\theta_M - tg\theta_A)^2 (\psi / tg\theta_M)^2$$

T. Wroblewski et al

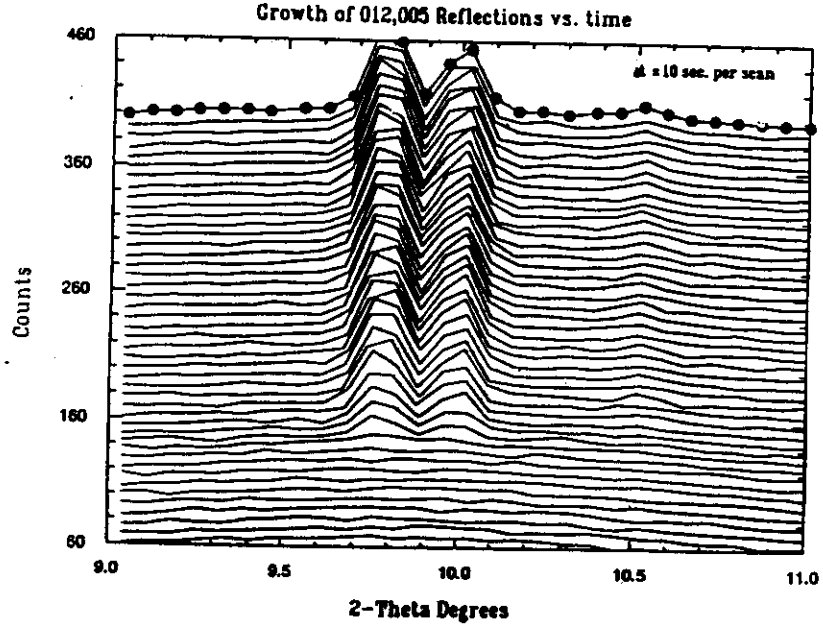


## Diffraction Chamber

T. Wroblewski et al

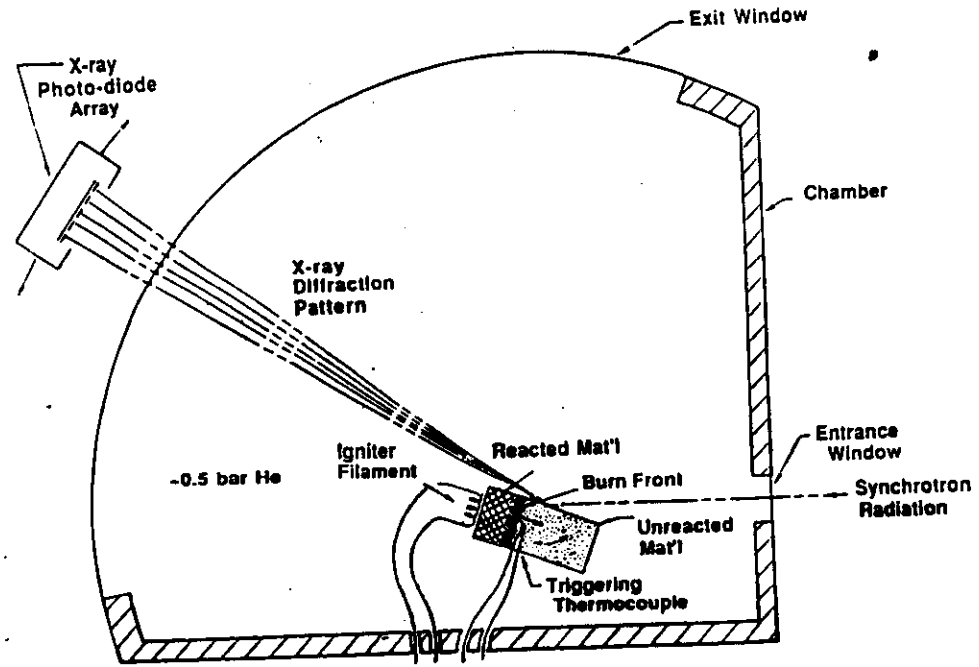

T. Wroblewski et al

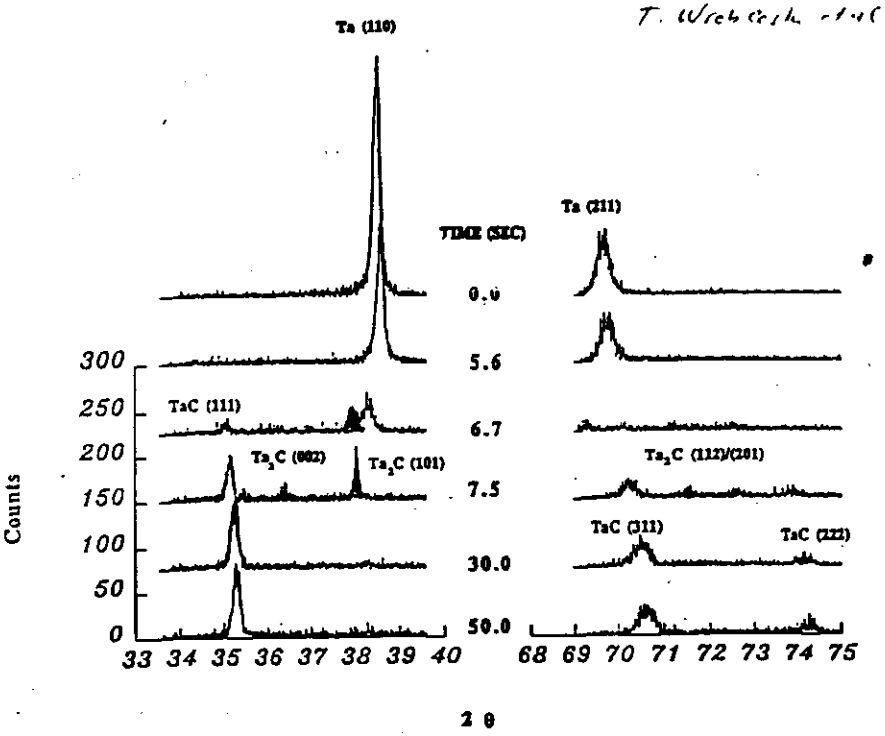


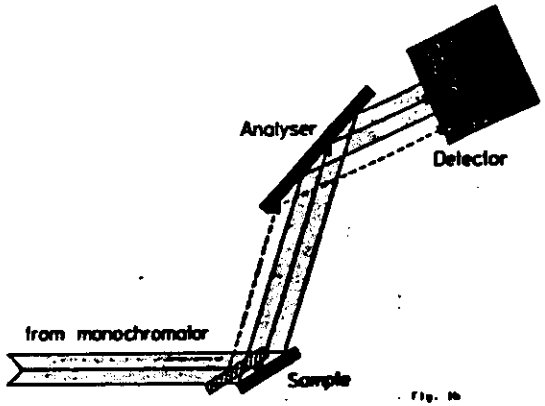


Fig. 1b

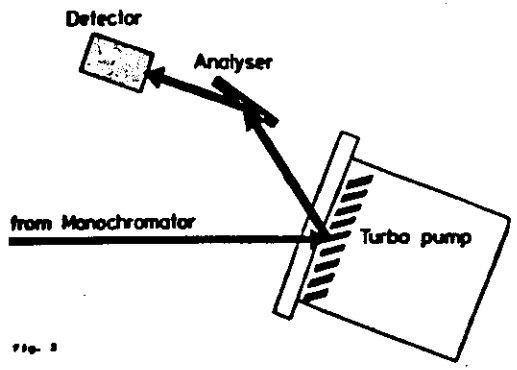


Fig. 2

J. Ihringer
A. Küster
J. K. Maichle
} Tübingen
T. Wroblewski

# X-ray Diffraction at high Pressure

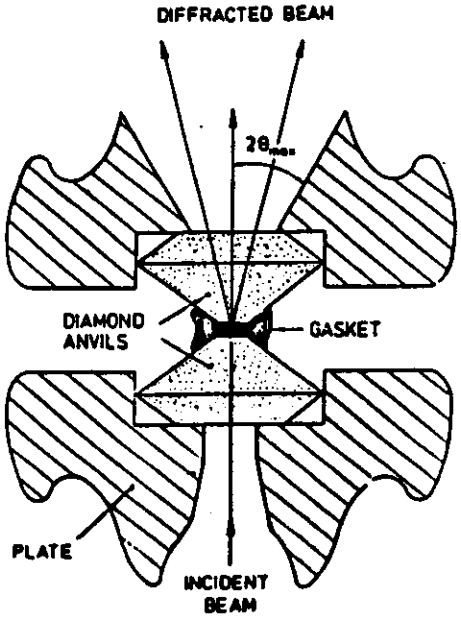


T. Wroblewski et al

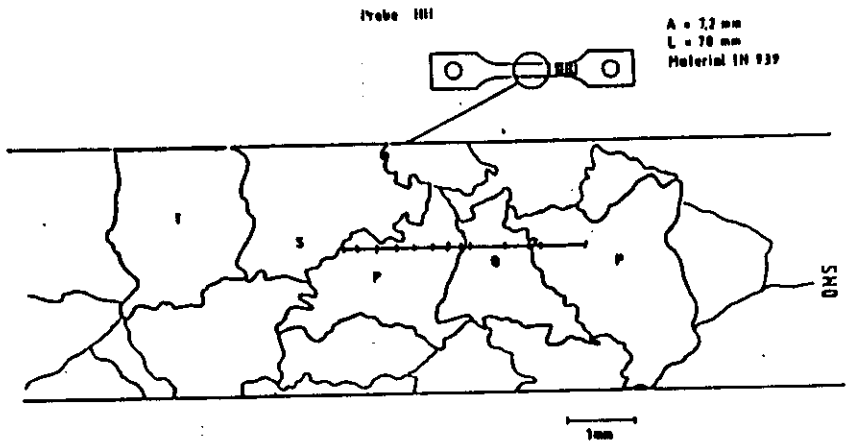


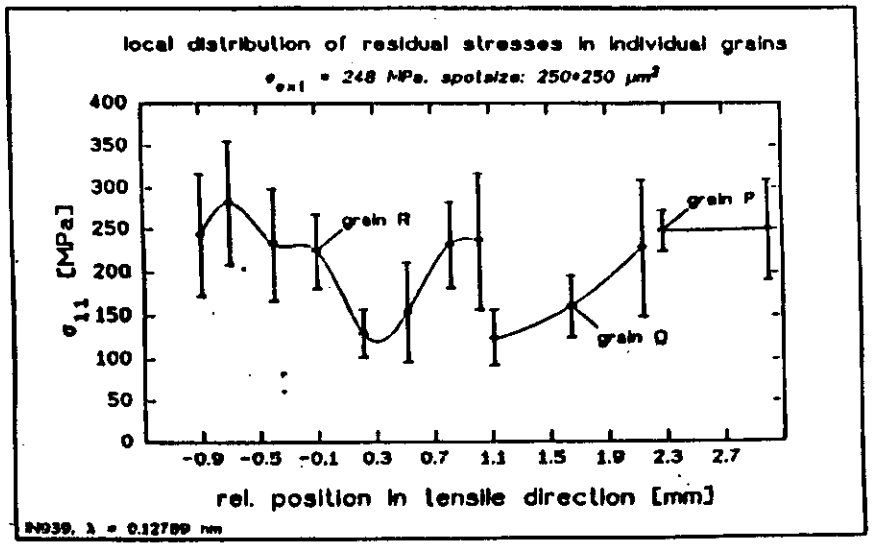

## X-ray Scattering by Amorphous Materials

$$A(q)_{e\ell} = a_e \qquad a_e = 7{,}9.10^{-26}\,\frac{1+\cos 2\theta}{2}$$

$$dA(\vec{q}) = \rho\, d\, v\, e^{-i\vec{q}\vec{r}}$$

$$A(\vec{q}) = \int \rho(r) e^{-i\vec{q}\vec{r}}\, dv$$

$$= \sum_R \int \rho(\vec{r}-\vec{r}) e^{-i\vec{q}(\vec{r}-R)}\, e^{-i\vec{q}\vec{R}}\, dV$$

$$= \sum_R f(q) e^{-i\vec{q}\vec{R}}$$

$$= f(q) \sum_R e^{-i\vec{q}\vec{R}}$$

$$I(q) = \underbrace{f^2}\ \underbrace{\left|\sum_R e^{-i\vec{q}\vec{R}}\right|^2}$$

Depends on the type of atom Atomic factor

Depends on the geometrical distribution of atomic centers Structure function = S(q)

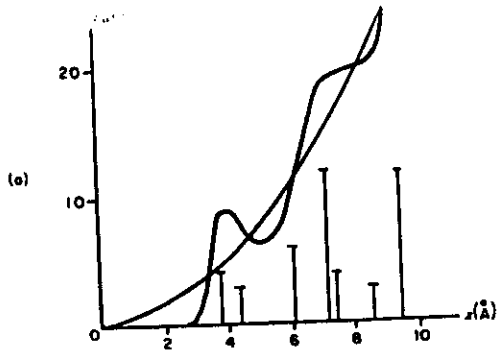


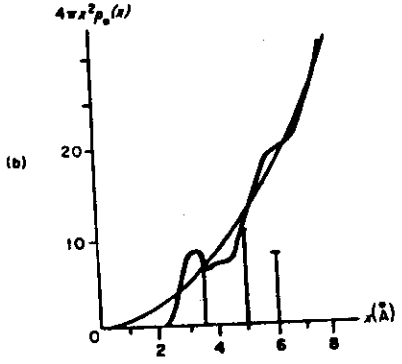


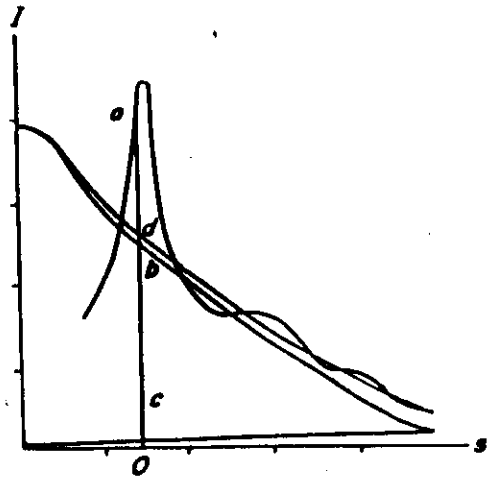


$$\sum_r e^{-i\vec{q}.\vec{R}} \equiv \int \rho(\vec{u}) e^{-i\vec{q}.\vec{u}}\, d\vec{u}$$

$$= \frac{1}{n} \iint \rho(\vec{u})\, \rho(\vec{u}')\, e^{-\vec{i}\, q(\vec{u}'-\vec{u})}\, d\vec{u}\, d\vec{u}'$$

$$\vec{u}' - \vec{u} = r$$

$$S(\vec{q}) = \int \underbrace{\left[\frac{1}{n} \int \rho(\vec{u})\, \rho(\vec{u}+\vec{r})\, d\vec{u}\right]}_{P(\vec{r})\text{: autocorrelation function}} e^{-i\vec{q}.\vec{r}}\, d\vec{r}$$

$$\boxed{S(\vec{q}) = \int P(\vec{r})\, e^{i\vec{q}.\vec{r}}\, d\vec{r}}$$

$S(\vec{q})$: Structure function

Monoatomic systems: $S(\vec{q}) = \dfrac{I(\vec{q})}{f^2}$

$$I(\vec{q}) = \sum_k \sum_j \left[ \sum_{k,\ell} f_{k\ell} \cos \vec{q}.\vec{r}_{k\ell} \right] .$$

$$. \left[ \sum_{j,m} f_{jm} \cos \vec{q}.\vec{r}_{jm} \right] \cos\left[\vec{q}(R_k - R_j)\right]$$

$$\overline{I(q)} = \left\{ \overline{N}\, \overline{F^2}(q) + \overline{F(q)}^2 \sum_k \sum_{j \neq k} \overline{\cos\left[\vec{q}.(\vec{R}_k - \vec{R}_j)\right]} \right\}$$

$$\iint_{v\,v} \frac{\sin\left\{q\left|\vec{R}_k - \vec{R}_j\right|\right\}}{q\left|\vec{R}_k - \vec{R}_j\right|} P_{kj}\, d_{v_k}\, d_{v_j}$$

$$\overline{I(q)} = \overline{N}\, F^2(h) \left\{ 1 - \frac{1}{v_1} \int_o^\infty [1 - P(r)] \frac{\sin qr}{qr} 4\pi r^2\, dr \right\}$$

$$g(r) = 4\pi r^2\, P(r)$$

$$P(\vec{r}) = \int S(\vec{q}) e^{i\vec{q}.\vec{r}}\, d\vec{q}$$

We define:

$$P(\vec{r}) = \delta(\vec{r}) + g(\vec{r})\rho_\circ$$

Where $\rho_O$ is the average atom density.

g $(\vec{r})$ is called reduced radial distribution function:

$$g(\vec{r}) = 0 \; for \; r < 2\, R_{at}$$

$$g(\vec{r}) = 1 \; for \; r >> R_{at}$$

$$P(\vec{r}) = \delta(\vec{r}) + (g(\vec{r}) - 1)\rho_\circ + \rho_\circ$$

$$\therefore S(\vec{q}) = \int \delta(\vec{r})\, e^{-i\vec{q}.\vec{r}}\, d\vec{r} + \rho_\circ \int [g(\vec{r}) - 1] e^{-i\vec{q}.\vec{r}}\, d\vec{r} +$$

$$+ \rho_\circ \int e^{-i\vec{q}\vec{r}}\, d\vec{r}$$

$$S(\vec{q}) = 1 + \rho_\circ \int [g(\vec{r}) - 1]\, e^{-i\vec{q}.\vec{r}}\, d\vec{r}$$

$$S(\vec{q}) - 1 = \rho_\circ \int [g(\vec{r}) - 1] e^{-i\vec{q}.\vec{r}}\, d\vec{r}$$

For isotropic systems

$$S(q) - 1 = \rho_\circ \int_\circ^{\alpha} \int_\circ^{2\pi} \int_\circ^{\pi} [g(r) - 1]\, e^{-iq.r\cos\theta}.$$

$$.\sin\theta\, d\theta\, r^2\, dr$$

$$q[S(q) - 1] = 4\pi\rho_\circ \int_\circ^{\infty} r[g(r) - 1] \sin qr\, dr$$

$$r[g(r) - 1] = \frac{1}{2\pi\rho_\circ} \int_\circ^{\infty} q[S(q) - 1] \sin qr\, dq$$

$\rho_\circ\, g(r)\, 4\pi r^2\, dr$: *number of atoms with center between r and r + dr*

$$\boxed{\rho_\circ\, g(r)\, 4\pi\, r^2 \Rightarrow R\,D\,F}$$

Binary systems

$$q[S_{ij}(q) - 1] = 4\pi \int_\circ^{\infty} r[g_{ij}((r) - 1)] \sin qr\, dr$$

$$r[g_{ij}(q) - 1] = \frac{1}{2\pi^2\rho_\circ} \int_\circ^{\infty} q[Sij(q) - 1] \sin qr\, dq$$

$$I(q) = \langle f^2 \rangle - \langle f \rangle^2 + \sum_{ij} c_i\, c_j\, f_i^*\, f_j\, S_{ij}(q)$$

ı the case of monoatomic systems:

$$\left.\begin{aligned} &< f^2 > = < f >^2 = f^2 \\ &I(q) = f^2 S_{11} \rightarrow S_{11} = \frac{I(q)}{f^2} \end{aligned}\right]$$

f we define the <u>total</u> structure function as follows:

$$S(q) = \frac{I(q) - \left[< f^2 > - < f >^2\right]}{< f >^2}$$

$$S(q) = \sum_{ij} W_{ij}(q)\, S_{ij}(q)$$

where $$W_{ij}(q) = R_e\left[\frac{c_i\, c_j\, f_i^*\, f_j}{< f >^2}\right]$$

$S_{ij}(q)$ are the <u>partial</u> structure functions

<u>Determination of the partial structure function</u>

Anomalous or resonant contribution to the atomic factor

$$f(q,E) = f_\circ(q) + f'(E) + if''(E)$$

$$[S] = \begin{vmatrix} S^1 \\ S^2 \\ S^3 \end{vmatrix}$$

$$[W] = \begin{vmatrix} W_{11}^1 & W_{12}^1 & W_{22}^1 \\ W_{11}^2 & W_{12}^2 & W_{22}^2 \\ W_{11}^3 & W_{12}^3 & W_{22}^3 \end{vmatrix}$$

$$[S_{ij}] = \begin{vmatrix} S^{11} \\ S^{12} \\ S^{22} \end{vmatrix}$$

$$[S] = [W][S_{ij}]$$

$$\therefore S_{ij} = [W]^{-1}[S]$$

- Conditionning:

$$(\bar{I}) = (\bar{A})(\bar{S})$$

$$\frac{\|\Delta S\|}{\|S\|} \leq \|W\| \left\|W^{-1}\right\| \frac{\|\Delta I\|}{\|I\|}$$

$$\left\|A_{ij}\right\| = \|F\| \left\|F^{-1}\right\|$$

$$\|A\| = \left(\sum_{ij} a_{ij}^2\right)^{1/2}$$

$$W_{nx3} = U_{nxn}\, A_{nx3}\, U_{3x3}^T$$

$$\begin{pmatrix} 0 & 0 \\ \sigma_2 & 0 \\ 0 & \sigma_3 \\ 0 & 0 \\ 0 & 0 \end{pmatrix}$$

Differential anomalous scattering

Binary system

$$I(q,E_1) = < f^2 >_1 - < f >_1^2 + c_A^2 |f_A|_1^2 \, S_{AA} +$$

$$+2\, c_A \, c_B \, R_e \left[ f_A \, f_B^* \right]_1 S_{AB} + |f_B|_1^2 \, S_{BB}$$

$$E_1 << >> E_{K_A}$$

$$E_1 << >> E_{K_B}$$

$$E_2 \equiv E_{K_A} \rightarrow (f_B)_1 = (f_B)_2$$

$$I(q,E_2) = < f^2 >_2 - < f >_2^2 + c_A^2 |f_A|_2^2 \, S_{AA}$$

$$+ 2\, c_A \, c_B \, \mathrm{Re} \left[ f_A \, f_B^* \right]_2 S_{AB} + |f_B|_2^2 \, S_{B_B}$$

$$\Delta I(q,E_1,E_2) = \Delta < f^2 > - \Delta < f >^2 + c_A^2 \, \Delta |f_A|^2 \, S_{AA} \cdot$$

$$2\, C_A \, C_B \, \Delta \, \mathrm{Re}\left[ f_A \, f_B^* \right]$$

$$S^{diff}\,(q, E_1, E_2) = \frac{\Delta I - \Delta < f^2 > + \Delta < f >^2}{\Delta < f >^2}$$

The Fourier transform provides

$$4\pi\, r^2 \; g_A(r) = 4\pi\rho_\circ + \frac{2r}{\pi} \int q \left( S^{diff} - 1 \right) \sin qr \; dq$$

$$= 4\pi\, r^2 \left[ \frac{\bar{f}_A}{< f >} \, g_{AA}\,(r) + \frac{f_B}{< f >} \, g_{AB}\,(r) \right]$$

Comparison DAS - EXAFS: These two aprroaches are complementary

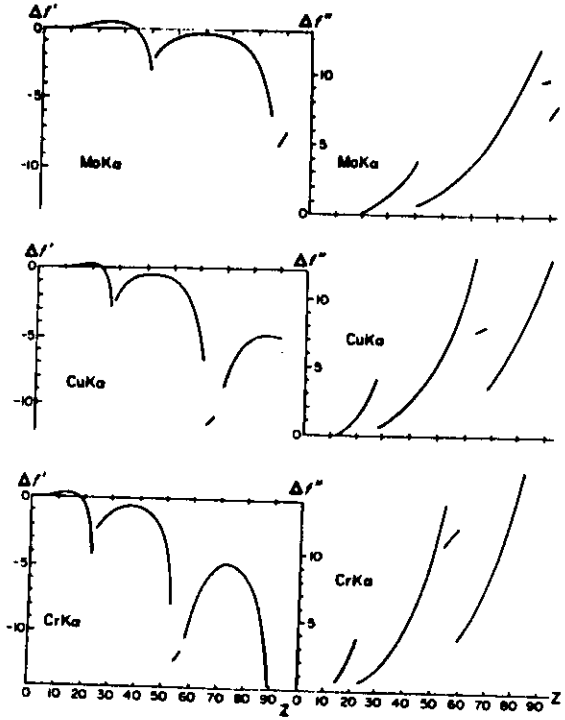

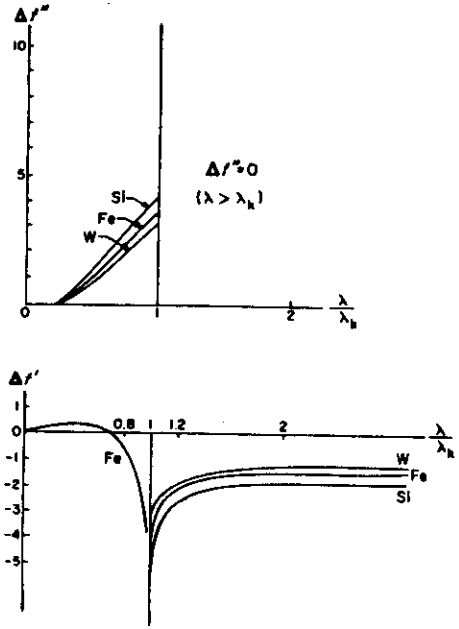


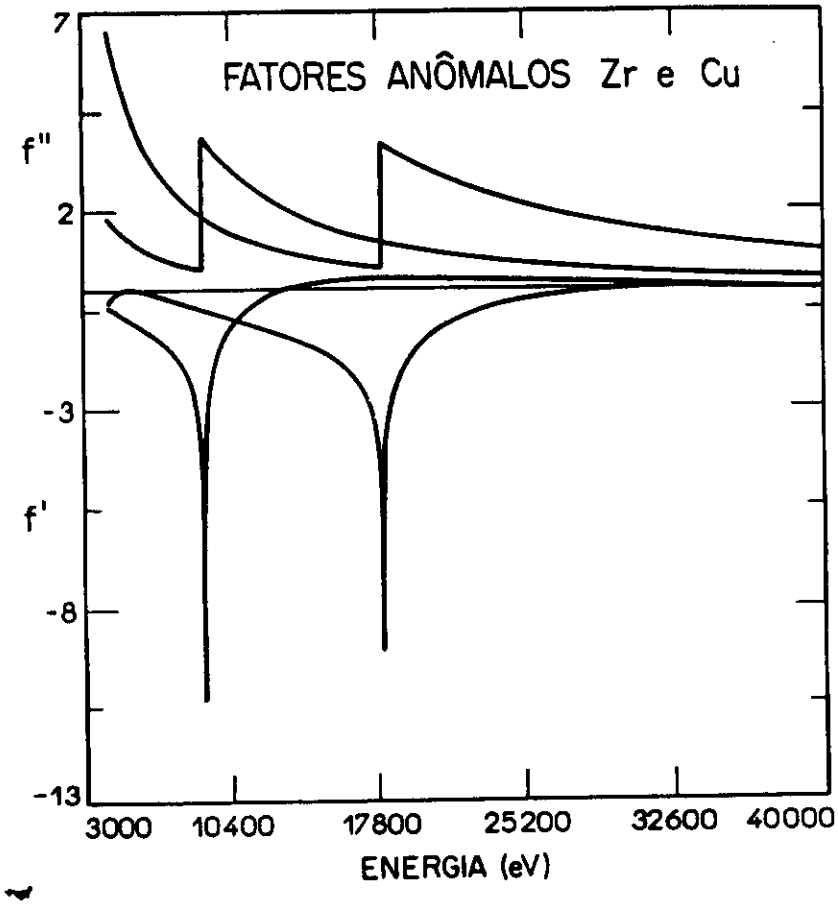


FIGURA II.12. Fatores de espalhamento anômalo ( f'(E) e f''(E) ) para os elementos Zr e Cu.

# AWAXS

## Experimental requirements

- Energy resolution: $\frac{\Delta E}{E} \langle 10^{-3}$

- Energy stability < 1 eV

- High flux to allow recording within a reasonable time interval.

Normally wiggler beam-lines and sagital focussing are used.

- Energy resolving X-ray detectors Si(Li) solid state detectors $\Delta E \approx 200$ eV at E = 7000 eV.

- Experimental setup:
  Two-circle diffractometer working in the vertical plane (horizontal axis).

## Data analysis

Normalization of intensity to absolute units involves several corrections.

- for nonlinearities of the detector

- for time decrease in incident beam intensity

- for a geometric form factor

- for sample absorption

- for fluorescence contribution

- for polarization

- for contribution from the substract

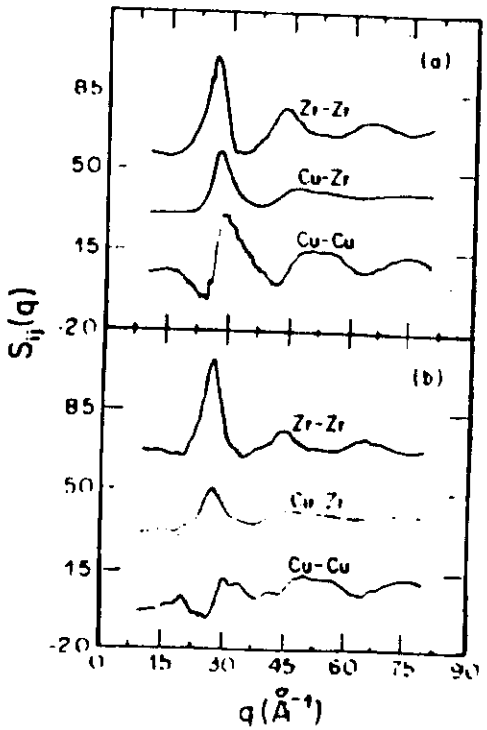


g. 5. (a) Refined PSFs of the anomalous set. (b) PSFs of the isomorphic set.

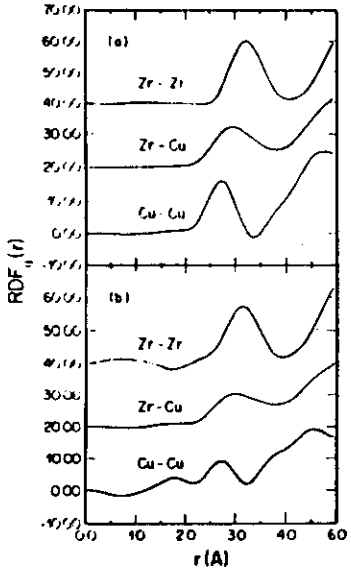


Fig. 7. Partial radial distribution functions of the anomalous (a) and isomorphic (b) set.

Table 2
Results obtained in this work (anomalous and isomorphic sets) compared with those of other authors

| | $D_{ij}$ values | | | $Z_{ij}$ values | | | | $\eta$ ($\eta_{ZrCu}$) |
|---|---|---|---|---|---|---|---|---|
| | ZrZr | ZrCu | CuCu | ZrZr | ZrCu | CuZr | CuCu | |
| Anomalous set | | | | | | | | |
| $Zr_{64}Cu_{36}$ | 3.20 ± 0.05 | 2.81 ± 0.05 | 2.63 ± 0.05 | 7.7 ± 0.3 | 4.5 ± 0.3 | 5.3 ± 0.3 | 4.7 ± 0.3 | −0.10 |
| Isomorphic set | | | | | | | | |
| $Zr_{64}Cu_{36}$ | 3.20 ± 0.05 | 2.85 ± 0.05 | 2.70 ± 0.05 | 10.3 ± 0.5 | 4.1 ± 0.5 | 4.8 ± 0.5 | 3.9 ± 0.5 | 0.00 |
| Ref. [8] | | | | | | | | |
| $Zr_{64}Cu_{36}$ | 3.15 | 2.75 | 2.53 | 5.0 | 5.6 | 5.6 | 5.8 | 0.019 |
| Ref. [22] | | | | | | | | |
| $Zr_{64}Cu_{36}$ | 3.15 | 2.80 | 2.65 | 5.9 | 6.7 | 5.0 | 5.4 | 0.014 |
| Ref. [23] | | | | | | | | |
| $Zr_{64}Cu_{36}$ | 3.28 | 2.77 | 2.59 | 5.2 | 6.7 | 5.1 | 8.2 | 0.056 |
| Ref. [24] | 3.20 | 2.84 | 2.56 | 10 | 3.2 | 7 | 4.4 | −0.21 |
| $Zr_{50}Cu_{50}$ | | | 3.20 | | | | | |
| Ref. [25] | 3.19 | 2.71 | 2.54 | 4 | 3.5 | 6 | 3.5 | 0.046 |
| $Zr_{33}Cu_{67}$ | 3.43 | | 3.05 | 3 | | | 1.5 | |

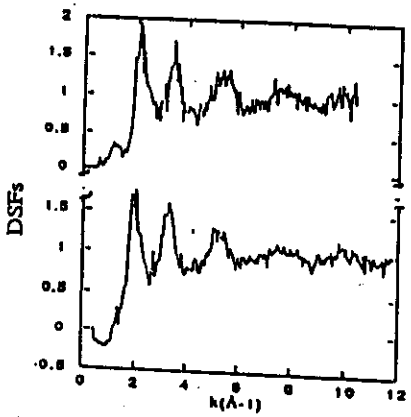


Fig. 1. The difference structure factors (DSF) of the As2Te3 glass obtained around the As (above) and Te (bottom) K edges, respectively

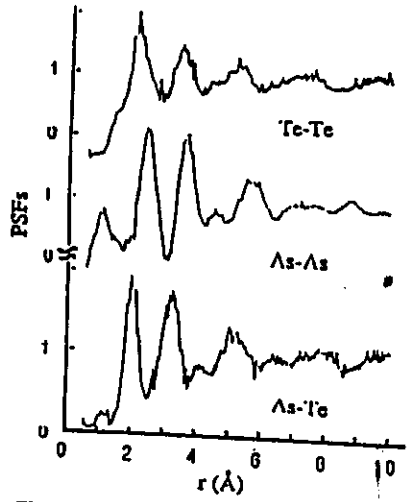


Fig. 3. The partial structure factors (PSF) of the As2Te3 glass

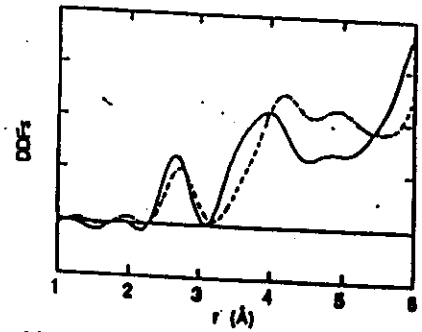


Fig. 2. The difference radial distribution functions (DDF) of the As2Te3 glass obtained around the As (full line) and Te (dashed line) K edges, respectively .

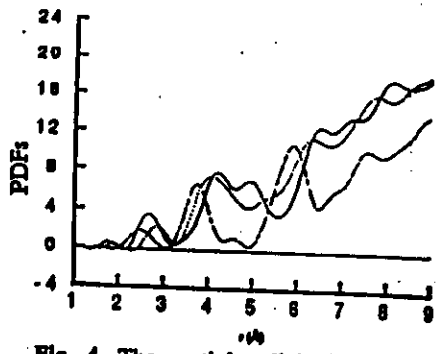


Fig. 4. The partial radial distribution functions (PDF) of the As2Te3 glass: As-As pairs (dashed line), As-Te pairs (full line), and Te-Te pairs (dotted line)

COMPARAISON OF PSF's OBTAINED USING ANOMALOUS X-RAY SCATTERING (J.C. De LIMA) AND USING NEUTRON SCATTERING IN AN EXTREMELY FAVORABLE* CASE (S. LEFEBVRE)

$Ni_2Zr$

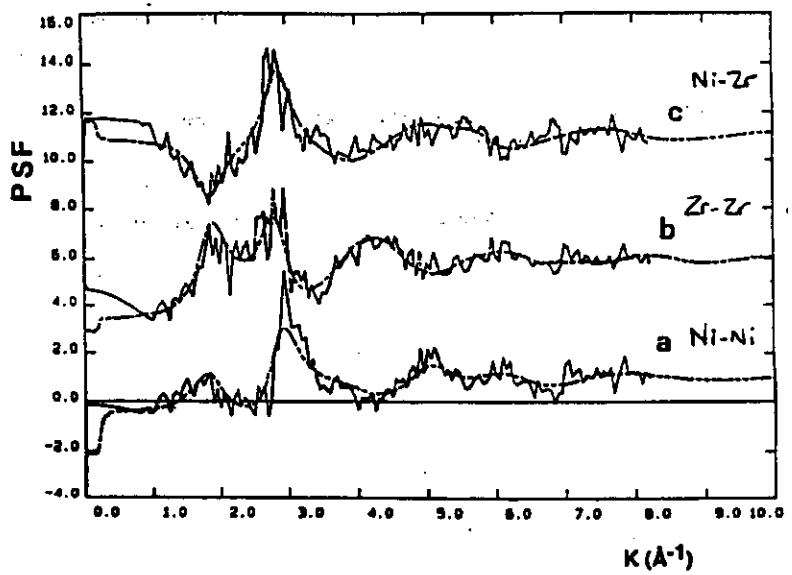


Figure IV-8 : Facteurs de structure partiels : a) Ni-Ni b) Zr-Zr c) Ni-Zr

2 TSF's + Zr-TSF's

Raw

rmally, as pointed out by Kortright et al. the informations
u can obtained are similar :

$$S_A^{diff}(q) = \sum_\alpha \frac{\bar{f}_\alpha(q,E)}{\langle f(q,E)\rangle} \int 4\pi \rho_{A\alpha}(r)\, r \sin qr\, dr$$

$$\chi_A(k) = \sum_\alpha -\frac{1}{k} S_0(k) \left|f_\alpha(k,\pi)\right| \int 4\pi \rho_{A\alpha}(r) \sin\left[2kr + \phi_{A\alpha}(k)\right] e^{\frac{-2r}{\lambda_\alpha(k)}} e^{-2\sigma^2 k^2}$$

Amplitude term in both formalism

EXAFS backscattering amplitude allows more chemical sensitivity

Atomic Scattering factors are only proportional to

The main difference → MEAN FREE PATH.
limits the spatial extension of the structural information.

The k-range accessible are quite different but complementary

Kortright et al

For disordered materials.

EXAFS → sharpest features
→ very nearest neighbors

However → some progress → Filipponi

DAS → medium range order

r multicomponent disordered
mple.

EXAFS easy to do, tricky to analyse

DAS ( reverse )

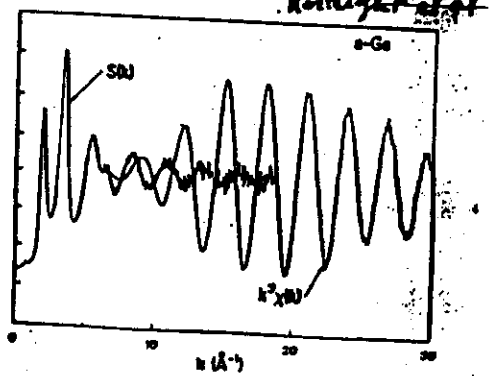


FIG. 14. Reciprocal-space oscillations from scattering and EXAFS are superimposed for amorphous Ge. The $k^2$ scale of EXAFS has been multiplied by 2 for comparison with the scattering data, but EXAFS phase shifts have not been removed. In the region of overlap and at higher $k$, these interference oscillations result from only the sharp, first-neighbor distance.